Fatigue behaviour of AISI 304 steel to AISI 4340 steel welded by friction welding

A. HASÇALIK*, E. ÜNAL
Department of Machine Education, Faculty of Technical Education, University of Firat, 23119 Elazığ

N. ÖZDEMIR
Department of Metal Education, Faculty of Technical Education, University of Firat, 23119 Elazığ

Published online: 12 April 2006

In the presented study, The weldability of AISI 304 austenitic stainless steel to AISI 4340 steel joined by friction welding in different rotational speeds and fatigue behaviour of friction-welded samples were investigated. Tension tests were applied to welded parts to obtain the strength of the joints. The welding zones were examined by scanning electron microscopy (SEM) and analyzed by energy dispersive spectroscopy (EDS). The Vıckers microhardness distributions in welding zone were determined. Fatigue tests were performed using a rotational bending fatigue test machine and the fatigue strength has been analysed drawing S-N curves and critically observing fatigue fracture surfaces of the tested samples. The experimental results indicate that mechanical properties and microstructural features are affected significantly by rotation speed and the fatigue strength of friction-welded samples decrease due to chromium carbide precipitation in welding zone with increasing rotation speed in choosen conditions.

1. Indroduction

Austenitic stainless steels and AISI 4340 steels are widely used in engineering applications for fabrication of structural components, in which high corrosion resistance and strength are fundamental design requirements respectively. In order to achieve combine properties of these materials, development of reliable joints between AISI 4340 and austenitic stainless steel is required to many applications. The welding of stainless steels and the properties of the welds with regard to corrosion resistance and mechanical properties do involve a mixture of metallurgical, geometrical and surface finishing aspect. The ability to join austenitic steels itself and to other materials with conventional fusion welding process such as gas tungsten, laser, electron beam welding opens up the possibility to product unexpected phase propagation and a series of negative metallurgical change such as delta ferrite phase, grain boundary corrosion, strain corrosion and sigma phase occurs at the welding interface. Therefore, extensive care and precautions like pre and post heat treatment or quick welding speeds are required [1–5]. These problems have been addressed by solid state welding processes, such as friction welding. Friction welding finds wide spread industrial use as a mass production process for the joining of materials. In welding process, the joining surface of samples are heated to the desired temperature through frictional heat and then a forging pressure is indroduced to weld the parts. Friction welding can be used to join metals of widely differing thermal and mechanical properties. Often combinations that can be friction welded can not be joined by other welding technigues because of the formation of brittle phases which make the joint poor in mechanical properties [6, 7]. Friction welding has been proven practical to eliminate the formation of the intermetallic phases and to form a sound weld [8, 9]. The sub-melting temperatures and short weld times of friction welding allow many combinations of work metals to be joined. The optimum welding parameters were chosen corresponding to the experience [10], the fracture in each test of tension specimens were outside the weld plane [11]. In order to optimise welding conditions for materials with different properties or advanced materials, experimental investigations are still required. Along with a great deal of research about

*Author to whom all correspondence should be addressed.
0022-2461
DOI: 10.1007/s10853-005-5478-7

TABLE I Chemical composition of parent metals (wt.%)

Composition	C	Si	Mn	P	S	Cr	Ni	Mo
AISI 4340	0.425	0.343	0.692	0.014	0.007	0.850	1.461	0.220
AISI 304	0.033	0.480	1.324	0.037	0.005	19.500	7.370	0.313

the weldability of dissimilar materials and properties estimation for friction welding process continuing, the further investigation on practical applications of failure is also becoming considerably important and urgent. It is well known that the majority of failures that occur in the structures are caused by fatigue failure in weldments due to fatigue type of loading experienced by the structures [12]. Very few studies have been carried out to evaluate the fatigue properties of AISI 304 stainless steel weld [13]. The fatigue process and its mechanism are largely influenced by the presence of material non-homogenities. It has been found by several researchers that generally fatigue cracks originate either in the heat affected zone or in the weld materials due to fatigue loading and could be the potential source of catastrophic failures in some unfortunate situations [14]. The aim of this study is to investigate experimentally the interface properties and fatigue behaviour in terms of rotational speed in friction–welded AISI 304 to AISI 4340 alloy steel.

2. Materyal and method

The composition of AISI 4340 steel and AISI 304 stainless steel used in experiments is given Table I. Each pair of work pieces (10 mm diameter and 60 mm length) faced on the mating ends was welded on the direct drive friction welding machine. In experiments, rotation speeds of 1500, 1800 and 2100 rpm were used. Friction pressure (30 Mpa), forging pressure (50 Mpa), friction time (6 s) and forging time (3 s) were fixed. The welded bars for fatigue specimens were worked with a CNC lathe and the weld interface was located in the middle of specimens. Finally, they were finished by polishing with emery papers of 600–1000 grit size.

Rotating bending fatigue tests were conducted using a sinusoidal load of frequency 50 Hz and load ratio $R = -1$, at room temperature, considering as fatigue strength, the complete specimens fracture or 2×10^6 load cycles. Eight groups of fatigue specimens were prepared to obtain S-N curves. Tensile testing was performed at room temperature using Instron type testing machine with 0,83 $\times 10^{-2}$ mm s^{-1} cross-head speed.

The welded interface was then cut longitudinally for investigating the structural properties. The integrity of the joints were examined by optical and scanning electron microscopy (SEM) for the microstructural changes. Energy dispersive spectroscopy (EDS) analyses were performed at both sides of the joints and microhardness profiles were measured across the friction welding joints. Fractography was also employed in evaluation of the fractured fatigue specimens.

3. Results and discussion

3.1. Microscopic examination

Fig. 1 shows microscopic cross-sectional view of samples welded at 1500, 1800 and 2100 rpm respectively. Microstructural evaluation of the friction welding joints

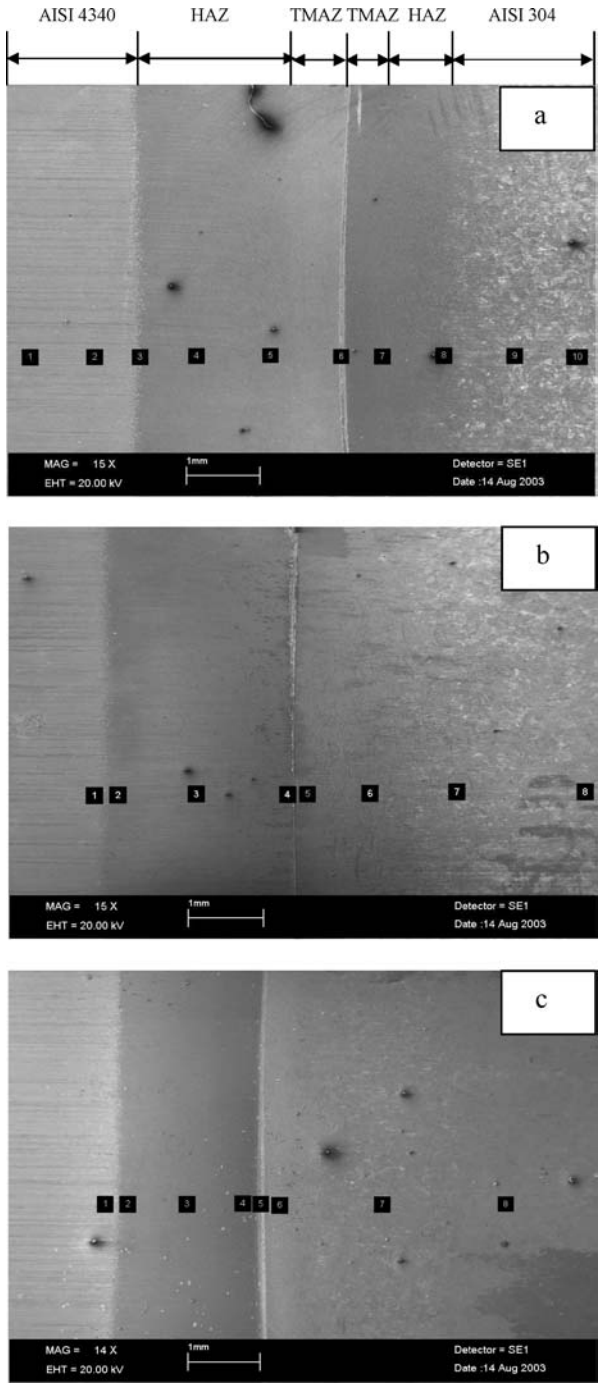

Figure 1 The macro SEM photo taken from welding zone of samples (a) 1500 rpm, (b)1800 rpm, (c) 2100 rpm.

revealed six distinct zone across the specimens which were identified as (1) parent AISI 4340 steel, (2) heat affected zone in the AISI 4340 steel side (HAZ), (3) termo-mechanically affected zone (TMAZ) in the AISI 4340 steel side, (4) termo-mechanically affected zone (TMAZ) in the AISI 304 steel side, (5) heat affected zone in the AISI 4340 steel side (HAZ), (6) parent AISI 304 steel. As can be seen from figures, the width of HAZ and TMAZ decreases with increasing rotational speed in both the AISI 4340 steel and AISI 304 steel. With increasing rotational speed, higher frictional heat causes to propagation of thermal energy along the axial direction of samples. A greater volume of material is therefore heated, leading to visco-plastic behaviour on the interface. The plastic incompressibility leads to the formation of flash, resulting to axial shortening. Typical microstructures from these regions are shown in Figs 2 and 3. The microstructure of the HAZ in the AISI 4340 steel consist of martensite phase. During the friction welding process, the temperature near the interface would reach between A_3 temperature and the melting point of AISI 4340 steel. When exposed to cooling from elevated temperatures, the AISI 4340 steel subject to a martensite transformation from austenite phase. The microstructure of the TMAZ in the AISI 4340 steel is similar to heat affected zone but this region was greatly deformed by the severe plastic deformation and frictional heat near the weld zone, resulting in fully martensite phase (Fig. 2).

The structure of parent AISI 304 steel shows typically coarse austenitic grains. The microstructure of the HAZ in the AISI 304 steel nearly exhibits similar structure to the base AISI 304 steel, but grains have been smaller. The grains of AISI 304 steel in the TMAZ are also smaller due to high deformation and frictional heat (Fig. 3). The frictional heat is not influential on the grain growth during cooling time. As known that the long holding times at the austenitizing temperature make sure that the austenite has reached its equilibrium grain size. In friction welding, cooling times are relatively short, therefore the time spent by the TMAZ and HAZ above A_3 is only of a few seconds meaning that the austenite cannot reach its equilibrium grain size. The severe plastic deformation leads to the formation of the shear bands. While small martensite cluster are formed at low rotation speed, the number of shear bands and shear band intersections increased with the increase of rotation speed, resulting in partial martensite formation in the austenite matrix. The martensite phase is nucleated at the intersections of shear bands (Figs 4–6). The interface represented very complex feature which was characterized by the metal flow of two different layers (Fig. 7). Fig. 8 presents detail of the morphology of welding interface. The width of this reaction layer decreased slightly with increasing rotating speed and showed about 60 μm for 1500 rpm.

Figs. 9 and 10 illustrate the concentration profiles of elements measured by the EDS analysis from the regions marked in Figs. 1a and c respectively. As seen in these figures, The concentration of *C* in TMAZ of AISI 304 and AISI 4340 steels increased when the rotation speed was increased. According to these results, with increasing the rotation speed, *C* concentration increases in TMAZ of AISI 304 steel because of the carbon atoms are rapid diffuser and most of the *C* reacts with Cr to form

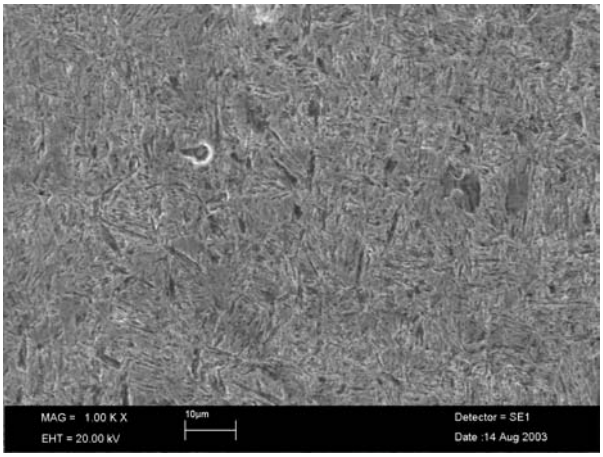

Figure 2 The microstructure of the TMAZ in the AISI 4340 steel.

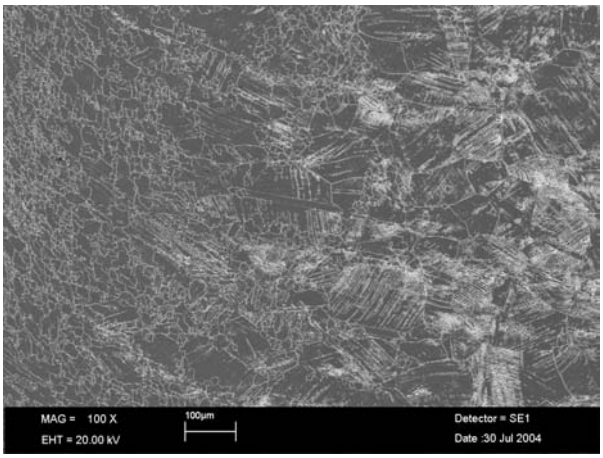

Figure 3 The microstructure of the TMAZ showing grain refinement in the AISI 304 steel.

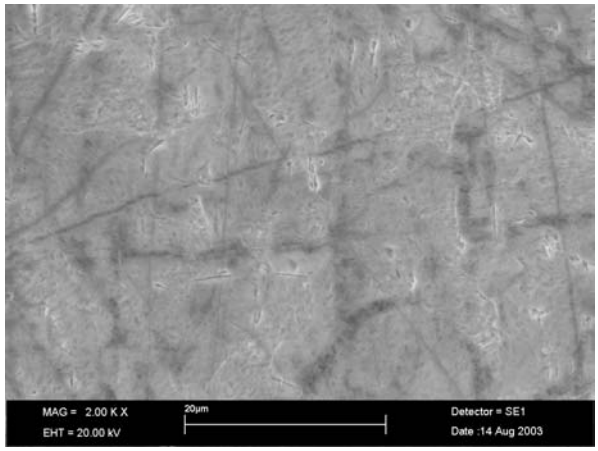

Figure 4 The microstructure of the TMAZ in the AISI 304 steel.

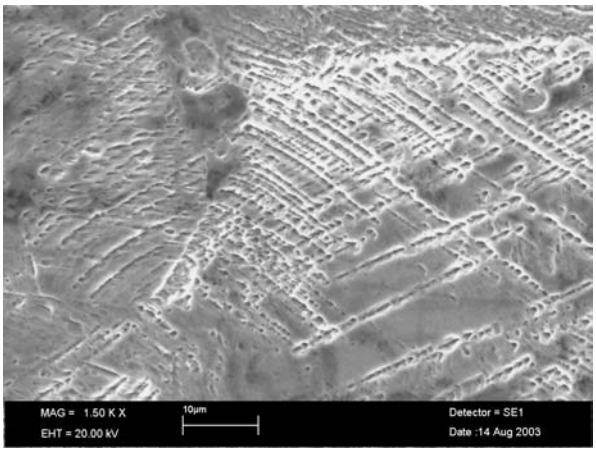

Figure 5 SEM observation of TMAZ for rotation speed of 1500 rpm in the AISI 304 steel.

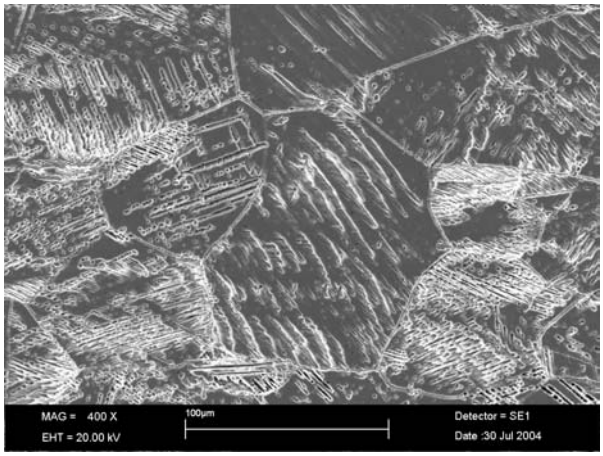

Figure 6 SEM observation of TMAZ for rotation speed of 2100 rpm in the AISI 304 steel.

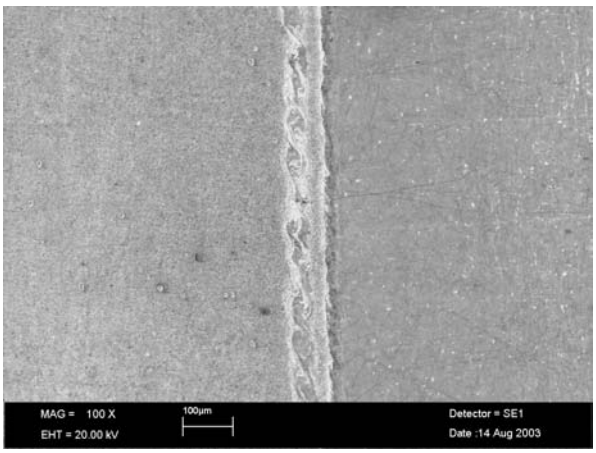

Figure 7 Macrographs of the friction weld interface for 1500 rpm.

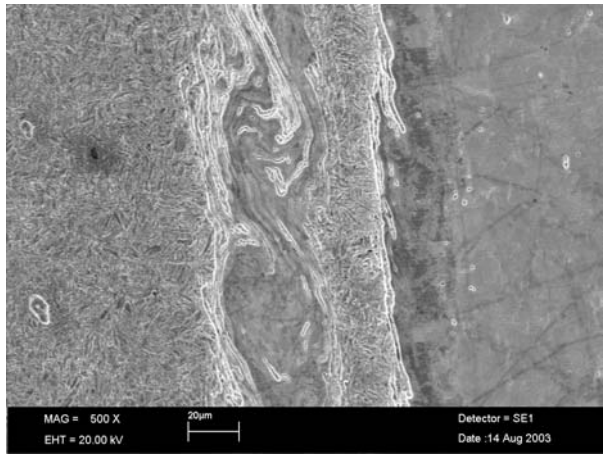

Figure 8 Magnified view of morphology of welding interface.

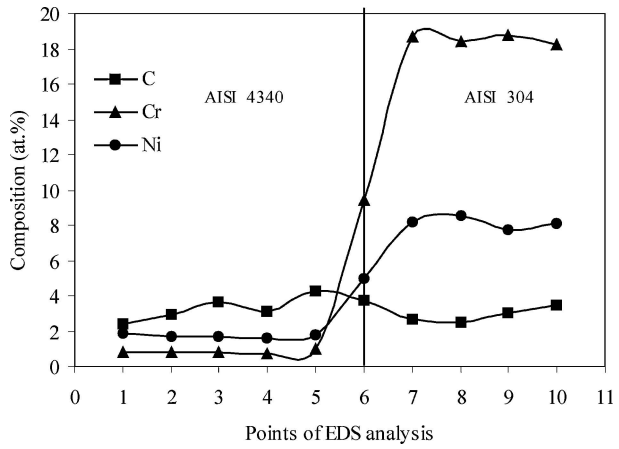

Figure 9 Concentration profiles of elements measured by the EDS analysis from the regions marked in Fig. 1a.

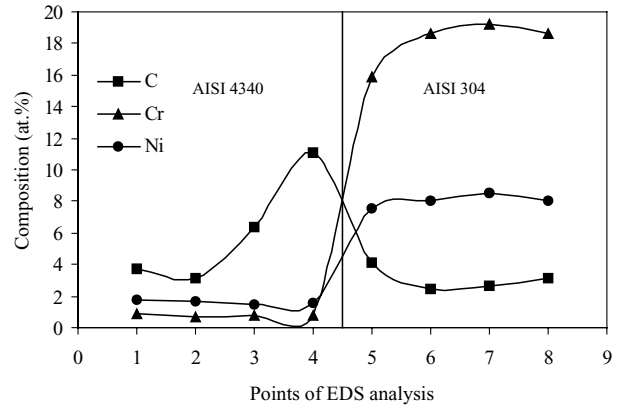

Figure 10 Concentration profiles of elements measured by the EDS analysis from the regions marked in Fig. 1c.

chromium carbides. As a consequence, the concentration of Cr in TMAZ of AISI 304 steel decreases relatively with increasing rotation speed. The precipitates formed are known to be M_3C_6 [15]. These results are attributed to the sufficient temperature and time to diffuse with increasing rotating speed in choosen conditions. İt is well known that exposure to the temperature range between 823 and 1073 K leads to precipitation of Cr-rich carbides directly associated with sensitization in austenitic stainless steels. The formation of Cr-rich carbides accompanies diffusion of Cr atoms to grain boundaries [16].

3.2. Microhardness and tensile test

Fig. 11 shows the cross-sectional hardness profile of the weld interface of friction-welded joints. As can be seen from this figure, almost the similar trend is observed in the microhardness profiles of all samples. The hardness of the HAZ and TMAZ increases with increasing rotational speed. The increasing hardness in the welding interface can be related directly to the microstructure formed in the welding interface as a result of the increasing heat input and plastic deformation. The increase in the hardness values in the AISI 304 side could be attributed to the work hardening of the austenitic stainless steel. It is widely accepted that work hardening of stainless steel is due to a martensite formation. Martensite may form in austenitic steels during plastic deformation from working (mechanical) or due to temperature effects (thermal) [17]. Although the deformation hardening is also effective on hardening in AISI 4340 steel side, mostly the hardening in this region is a direct result of the rapid cooling from the welding temperature. Hardness of AISI 4340 side near interface remarkably increased and reached approximately 1100 HV. This hardened region could be attributed to martensite structure (Fig. 2). This region reached approximately 1 mm from the weld interface to AISI 4340 steel side. This can be explained by the higher thermal conductivity of AISI 4340 steel which permits a rapid dissipation of the heat through the sample while AISI 304 steel retards dissipation of heat because of lower thermal conductivity. As a consequence, the lower hardness can be expected in AISI 4340 side adjacent to the AISI 304 steel.

Mechanical properties of the friction-welded samples are given in Table II. The tensile strength slightly decreased with increasing rotational speed. The fracture mainly occured at the AISI 304 steel side. Existing literature reports that, a higher bonding temperature results in profuse inter-diffusion and better coalescence of mating surfaces [18]. However increasing bonding temperature due to increasing rotation speed also promotes the growth of brittle intermetallics which, in turn affect the bond strength adversely. Therefore, the low values of elongation and tensile strength can be attributed to presence of aligned chromium precipitation which reduce this properties. According to Zhu et al. [19] such behaviour results from the elastic restraint imposed on the matrix by the particulate due to their elastic modulus difference and subsequent stress concentration around them.

TABLE II Mechanical properties of the friction-welded samples

Rotation speed (rpm)	Tensile strength (MPa)	Yield strength (MPa)	% Elongation (ε)
1500	896	628	24
1800	838	610	23
2100	822	590	20

3.3. Fatigue test

Fig. 12 shows the S-N curves for the rotation bending fatigue tests of the friction welded samples. As seen this figure, the fatigue endurance decreased with increasing the rotational speed. The fracture mainly occured at the deformed zone of AISI 304 steel side. This result can be explained by the formation of chromium carbide precipitation, which acts as a stress raiser. At high rotational speeds longer heating times are required allowing propagation of thermal energy along the axial direction of the workpieces. A greater volume of material is therefore heated, leading to lower cooling rates and wider transformed regions [20]. This leads to the sufficient temperature and time to diffuse of carbon to AISI 304 side. The diffusion of carbon to AISI 304 side causes to the formation of chromium carbide precipitation at the grain boundaries which are known to be deleterious to the fatigue life of material. The carbides at the grain boundaries provide preferential sites for cavity nucleation in austenitic stainless steels under fatigue conditions, thereby reducing the fatigue life [21, 22]. On the other hand, the extensive deformation in the deformed zone due to the increasing in the rotational speed could lead to build up of residual stresses. Higher residual stresses at the AISI 304 steel side of the interface can be attributed to the higher flow stress of the austenitic stainless steel. These residual stresses can

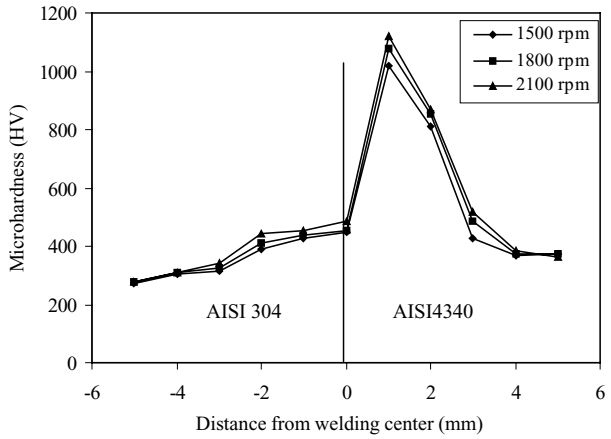

Figure 11 Microhardness distributions of friction-welded joints.

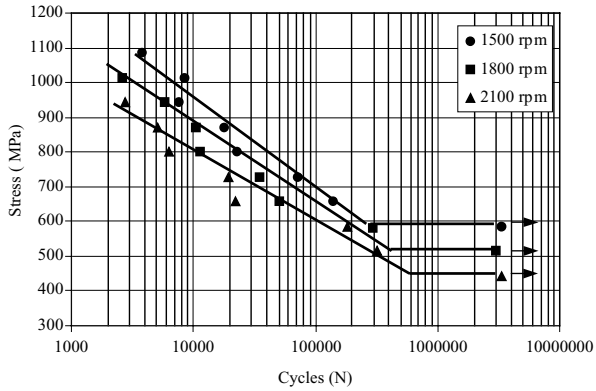

Figure 12 S-N curves of friction welded samples.

have a effect in the decrease of fatigue limit. The location of failure in all the cases was outside the interface but in the deformed zone of the AISI 304 steel next to the interface. Typical fractographs shown in Figs 13–15 show that fracture characteristic of all of the friction-welded samples is dominated by the ductile mechanism. In samples welded at 1500 rpm, fatigue striations formed during stage II propagation were observed (Fig. 13). Fatigue striations are the result of a sliding off or alternating shear process at the crack tip. In the sample welded at 1800 rpm, the observation of cracks could be associated with the partially transformed martensite phase in austenite matrix. Because of non-uniform microstructure, local stresses may be concentrated at these locations and may cause secondary fatigue cracks to initiate [23]. The fracture mode of samples welded at 2100 rpm dominated by the transgranular microvoid coalescence (Fig. 15). As known, the voids which are the basic source of ductile fracture are nucleated heterogeneously at sites where compatibility of deformation is difficult. The preferred sites for void formation are possibly second phase particles. The apparance of the fracture surface consist of different types of dimples and larger ones may result from chromium carbide precipitates.

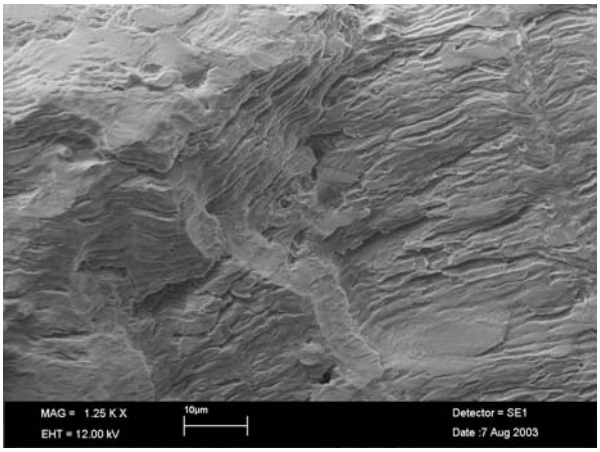

Figure 13 SEM fractograph showing fatigue striations of the sample welded at 1500 rpm.

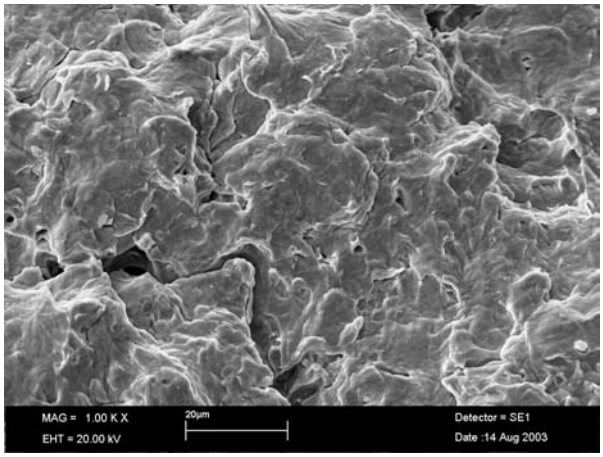

Figure 14 SEM fractograph of the sample welded at 1800 rpm.

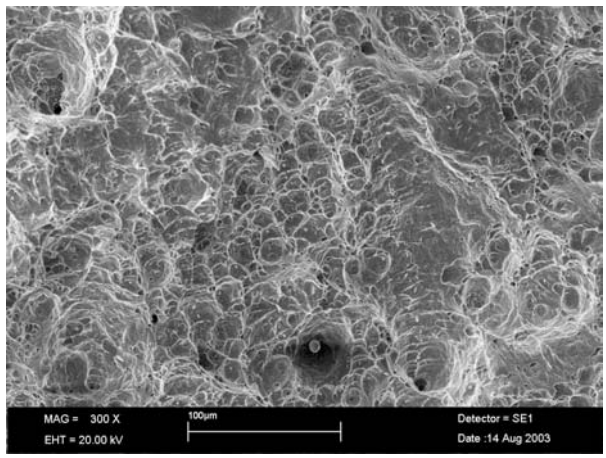

Figure 15 SEM fractograph of the sample welded at 2100 rpm.

4. Conclusions

In the presented study, the weldability of AISI 304 austenitic stainless steel to AISI 4340 steel joined by friction welding in different rotational speeds and fatigue strength of samples were investigated. Summarizing the main features of results of microstructure analysis, hardness, tensile and fatigue tests, the following conclusions may be drawn.

(1) The present study has demonstrated that AISI 304 stainless steel can be joined to AISI 4340 steel using friction welding. Microstructural evaluation of the friction welding joints revealed six distinct zone across the specimens which were identified as (1) parent AISI 4340 steel, (2) heat affected zone in the AISI 4340 steel side (HAZ), (3) termo-mechanically affected zone (TMAZ) in the AISI 4340 steel side, (4) termo-mechanically affected zone (TMAZ) in the AISI 304 steel side, (5) heat affected zone in the AISI 4340 steel side (HAZ), (6) parent AISI 304 steel.

(2) The hardness of the HAZ and TMAZ increases with increasing rotational speed as a result of the increasing heat input and plastic deformation. The increase in the hardness in the AISI 304 and AISI 4340 steel could be attributed to the work hardening and martensite phase respectively. The tensile strength and elongation also decreased with increasing rotational speed. The low values of elongation and tensile strength can be attributed to presence of aligned chromium precipitation

(3) The fatigue endurance decreases with increasing the rotational speed as result of formation of chromium carbide precipitation in choosen conditions. The fracture characteristic of all of the friction-welded samples is dominated by the ductile mechanism.

Acknowledgments

The support of the F. Ü. Scientific Research Project Department is gratefully acknowledged.

References

1. SEUNG HWAN and C. PARK, et.al., Corrosion resistance of friction stir welded 304 stainless steel, *Scripta Materialia* **51** (2004) 101.
2. C. R. DAS, A. K. BHADURI and S. K. RAY, Fatigue failure of a fillet welded nozzle joint, *Engineering Failure Analysis* **10** (2003) 667.
3. H. U. HONG, B. S. RHO and S. W. NAM, A study on the crack initation and growth from δ-ferrite/γ phase interface under continuous fatigue and creep-fatigue conditions in type 304L stainless steel, *International Journal of Fatigue* **24** (2002) 1063.
4. K. S. MIN, K. J. KIM and S. W. NAM, Investigation of the types and densities of grain boundary carbides on grain boundary cavitation resistance of AISI 321 stainless steel under creep-fatigue interaction, *Journal of Alloys and Compound* **370** (2004) 223.
5. E. J. RAO, B. GUHA, G. MALAKONDAIAH and V. M. RADHAKRISHNAN, Effect of welding process on fatigue crack growth behaviour of austenitic stainless steel welds in a low alloy steel, *Theoretical and Applied Fracture Mechanics* **27** (1997) 141.
6. A. VAIRIS and M. FROST, High frequency linear friction welding of a titanium alloy, *Wear.* **217** (1998) 117.
7. A. Z. ŞAHIN, B. S. YIBAŞ, M. AHMED and J. NICKEL, Analysis of friction welding process in relation to the welding of copper and steel bars, *Journal of materials processing technology* **82** (1998) 127.
8. S. SUNDARESAN and K. G. K. MURTI, The formation of intermetallic phases in aluminum-austenitic stainless steel friction welds, *Material Forum* **17** (1993) 301.
9. S. FUKUMOTO, T. INUKI, H. TSUBAKINO, K. OKITA, M. ARITOSHI and T. TOMITAL, Evaluation of friction weld interface of aluminum to austenitic stainless steel joint, *Material Science and Technology* **13** (1997) 679.
10. J. W. ELMER and D. D. KAUTZ, "Welding, Brazing and Soldering, ASM Handbook" (1994) Vol. 6 pp. 150.
11. H. BEHNKEN and V. HAUK, Micro-residual stresses caused by deformation, heat, or their combination during friction welding, *Materials Science and Engineering* **A289** (2000) 60.
12. P. JOHAN SINGH, B. GUHA and D. R. G. ACHAR, Fatigue life prediction for stainless steel welded CCT geometry based on Lawrance's local-stress approach, *Engineering Failure Analysis* **10** (2003) 655.
13. L. W. TSAY, Y. C. LIU, M. C. YOUNG and D. Y. LIN, Fatigue crack growth of AISI 304 stainless steel welds in air and hydrogen, *Materials Science and Engineering* **A374** (2004) 204.
14. M. A. WAHAP and M. SAKANO, Corrosion and biaxial fatigue of welded structures, *Journal of Materials Processing Technology* **143–144** (2003) 410.
15. P. ASOKA-KUMAR and J. H. HARDLEY, et. al., Direct observation of carbon-decorated defects in fatigued type 304 stainless steel using positron annihilation spectroscopy, *Acta Materialia* **50** (2002) 1761.
16. S. H. C. PARK, et.al., Corrosion resistance of friction stir welded 304 stainless steel, *Scripta Materialia* **51** (2004) 101.
17. D. O'SULLIVAN and M. COTTERELL, Machinability of austenitic stainless steel SS303, *Journal of Materials Processing Technology* **124** (2002) 153.
18. M. EROGLU, T. L. KHAN and N. ORHAN, Diffusion bonding between Ti-6Al-4V alloy and micro duplex stainless with copper interlayer, *Mater. Sci. Technol.* **18** (2002) 68.
19. S. H. ZHU, P. K. LIAW, J. M. CORUM, and H. E. MCCOY, Jr, High temperature mechanical behaviour of Ti-6A-4V alloy and TiC_p /Ti-6Al-4V composite, *Metall. Trans.* **A30** (1999) 1569.
20. A. M. SILVA ANTONIO, MEYER AXEL, F. DOS SANTOS JORGE, E. F. KWIETNIEWSKI CARLOS and T. E. STROHAECKER, Mechanical and metallurgical properties of friction welded TiC particulate reinforced Ti-6Al-4V, *Composites Science and Technology* **64** (2004) 1495.
21. H. U. Hong, B. S. Rhu, S. W. Nam, Correlation of the $M_{23}C_6$ precipitation morphology with grain boundary characteristics in austenitic stainless steel, *Materials Science and Engineering* **A318** (2001) 285.
22. BYUNG SUP RHO and SOO WOO NAM, Effects of nitrogen on low-cycle fatigue properties of type 304 L austenitic stainless steels tested with and without tensile strain hold, *Journal of Nuclear Materials* **300** (2002) 65.
23. J. C. NEWMAN, The merging of fatigue and fracture mechanics concepts; a historical perspective, *Fatigue and Fracture Mechanics* **8** (1997) 3 [ASTM STP 1321].

Received 13 May 2005
and accepted 12 July 2005